*Quaternary Research*

doi:10.1017/qua.2018.128

# Development of Quaternary travertines in the carbonate mountains of the western Costa del Sol, Málaga, southern Spain

Antonio Guerra-Merchán[a]*, Francisco Serrano[a], José M. García-Aguilar[a], José E. Ortiz[b], Trinidad Torres[b], Yolanda Sánchez-Palencia[b]

[a]Departamento de Ecología y Geología, Universidad de Málaga, Campus de Teatinos, 29071 Málaga, España
[b]Laboratorio de Estratigrafía Biomolecular, Escuela Técnica Superior de Ingenieros de Minas y Energía, Universidad Politécnica de Madrid, España
*Corresponding author e-mail address: antguerra@uma.es

(Received May 30, 2018; Accepted October 9, 2018)

**Abstract**

The predominantly carbonate nature of the mountains near the coast of Málaga and Marbella (Costa del Sol, southern Spain) and the presence of springs have favored the formation of travertine buildups during the Quaternary. The geomorphic characteristics of the slopes and the location of the springs have determined the development of three types of travertine growths: (1) spring travertines, located preferentially on the south mountainside, where the slope is steepest; (2) pool-dam-cascade travertines, which form along the north and east edges, far from the carbonate relief and with a gentler slope; and (3) river-valley travertines, formed in the courses of the springs of any sector. Field observations combined with new amino acid racemization (AAR) dating of Helicidae gastropods show that most of the travertine formations are polyphasic and that their development was interrupted by stages of erosion and incision. Five stages of travertine development are evident, most of which are related to warm, moist episodes corresponding to marine oxygen isotope stages (MIS) 7, 5, 3, and 1, although local travertine growth also occurred during MIS 6 and during the transition from MIS 3 to 2.

**Keywords:** Travertine; Gastropods; Amino acid racemization; Quaternary; Málaga; Costa del Sol; southern Spain

## INTRODUCTION

Travertines and/or calcareous tufas are sedimentary rocks of continental origin formed by the precipitation of calcium carbonate in areas where the water from springs, waterfalls, rivers, or lakes loses its carbon dioxide ($CO_2$) and calcite or aragonite precipitates (Pentecost and Viles, 1994; Pentecost, 2005). Some researchers use the term "travertine" in a broad sense without difference between travertine and tufa (Juliá, 1983; Hubbard and Herman, 1990; Pentecost, 1993; Pentecost and Viles, 1994), whereas others establish differences related to water temperature, the origin of the dissolved $CO_2$, the porosity, and/or the degree of compaction (Whitten and Brooks, 1972; Bates and Jackson, 1987; Pedley, 1990; Riding, 1991; Koban and Schweigert, 1993; Ford and Pedley, 1996; González Martín and González Amuchastegui, 2014). In general, for these latter researchers, travertines are of hydrothermal origin, while calcareous tufas originate from cold carbonate-rich waters. In agreement with Juliá (1983) and Pentecost (2005), we use the term travertine in the broad sense and include all limestones chemically precipitated in relation to fountainheads, springs, groundwater, fluvial currents, and, less frequently, lakes. These rocks are characterized by having low to moderate intercrystalline porosity and often high structural porosity.

Travertines usually develop at the foot of carbonate mountains that constitute aquifers and present frequent springs. Their study offers abundant information related to the hydrogeology of the aquifer, environmental conditions, climatic change, and geomorphic evolution (e.g., Henning et al., 1983; Magnin et al., 1991; Pentecost, 1995, 2005; Torres et al., 1996; Durán, 1996; Martín-Algarra et al., 2003; Delgado Castilla, 2009). Travertines can be chronometrically dated by different methods including electron spin resonance (ESR; e.g., Grün et al., 1988; Clark et al., 1991), methods related to the uranium/thorium series (U/Th; e.g., Hillarie-Marcel et al., 1986; Kronfeld et al., 1988; Durán, 1996; Eikenberg et al., 2001; Soligo et al., 2002), radiocarbon ($^{14}C$; e.g., Clark and Fontes, 1990; Srdoč et al., 1983),

**Cite this article:** Guerra-Merchán, A., Serrano, F., García-Aguilar, J. M., Ortiz, J. E., Torres, T., Sánchez-Palencia, Y. 2019. Development of Quaternary travertines in the carbonate mountains of the western Costa del Sol, Málaga, southern Spain. *Quaternary Research* 92, 183–200.

thermoluminescence (TL; e.g., Reddmann and Schüttlekopf, 1986; Engin and Güven, 1997), and amino acid racemization (AAR, e.g., Goodfriend, 1991; Torres et al., 1996, 2005; Kaufman and Manley, 1998; Kaufman, 2000; Ortiz et al., 2009). These dating methods help determine the nature of travertine development and its relation to paleoclimatology.

In southern Spain and particularly in the province of Málaga, the abundance of carbonate mountain ranges (sierras) favors the proliferation of travertine buildup (Durán, 1996; Durán et al., 1988; Rodrigo Comino and Senciales González, 2012). A clear example of this is the landscape of the western Costa del Sol (mainly the Sierra de Mijas and other minor sierras; Fig. 1A and B), in which travertines form steps on the sierra slopes and the presence of fountainheads and springs have encouraged the establishment of human settlements.

The main aim of this work is to establish the different sedimentary models and the chronology of the travertines developed in the study region. To this end, the geomorphic characteristics and the different facies in each travertine buildup are analyzed as are the inner erosive surfaces that differentiate growth phases. AAR dating based on the remains of gastropods (*Otala punctata* and *Theba pisana* belonging to family Helicidae) present in most of the travertine buildups were carried out to help establish the chronology. Previously available radiometric dating provided by Durán et al. (1988), Durán (1996), and Durán et al. (2002) is also considered in our study.

## Geologic and geomorphic context

The Sierra de Mijas is a mountain range oriented E-W within the western sector of the Internal Zone of the Betic Cordillera, southwest of the city of Málaga (Fig. 1A). This mountain range, formed by the Blanca Unit (Mollat, 1968), belonging to the Alpujarride Complex (Piles Mateo et al., 1978; Andreo and Sanz de Galdeano, 1994; Sanz de Galdeano, 1997), is composed mainly of marble (Fig. 1B). South of the massif, a narrow band of pelite formations belonging to the Blanca Unit crops out. These formations are some 100–500-m-wide and 400-m-thick and include migmatite, gneiss, and pale schist. These pelite are located stratigraphically below the marble, although they locally appear above it in tectonically-reversed position and represent the impermeable bottom of the carbonate aquifer of the Sierra de Mijas.

Towards the south and west of the Sierra de Mijas, the Blanca Unit is overthrust by peridotite and pelite (gneiss and micaschist with quartzite) belonging to the Alpujarride Los Reales Unit (Tubía, 1985; Sanz de Galdeano, 1997). This latter unit is overthrust by the Malaguide Complex made of Paleozoic phyllite, slate, greywacke, and contorted turbiditic limestone (*calizas alabeadas* facies) and Triassic red conglomerate, sandstone, and mudstone.

The north and east boundaries of the Sierra de Mijas are marked by oblique-slip and strike-slip faults that were active mainly during the lower and middle Miocene (Sanz de Galdeano and López Garrido, 1991), but they also show mainly dip-slip displacement when they affect the upper Miocene and Pliocene sedimentary rocks. Sierra de Mijas is also affected by a NW-SE to NNW-SSE faulting system with 70–85° dips towards the west and oblique throws. Two major faults of this system (the Arenales and Benalmádena faults; Insua-Arévalo, 2008; Guerra-Merchán et al., 2018) divide the mountain range into three sectors (Fig. 1B) in which the contact between the pelite and the marble is found at different heights, thus affecting the areas of travertine development.

The Sierra de Mijas presents a mountainous landscape with slopes ranging up to 35°. In the lower areas of the Sierra de Mijas, the slope is usually gentler due to the presence of remains of early Pliocene abrasion platforms (Rodríguez-Vidal et al., 2007; Insua-Arévalo, 2008). Up to three generations of Quaternary alluvial fans are present in the foothills of the Sierra de Mijas at different elevations (Insua-Arévalo et al., 2007, 2012; Guerra-Merchán et al., 2018) as well as multiple travertine buildups with different thicknesses and extents (Durán, 1996; Durán et al., 1988). These alluvial fans and travertine deposits result in a stepped landscape in the lower part of the Sierra de Mijas and along its boundaries.

## MATERIAL AND METHODS

We measured the amino acid content in 118 land snail shells belonging to the family of Helicidae that were collected from 20 travertine deposits within the study area. In most locations, land snails were *Otala punctata* (Müller, 1774), whereas *Theba pisana* (Müller, 1774) representatives were selected in four of them (Table 1; CHU-2, ALH-3, COI-2, COI-3). *Otala punctata* (Fig. 2A) is characterized by shells with a diameter ranging from 33 to 39 mm; the umbilicus is inconspicuous, and the peristome is slightly thickened with the aperture brown- to red-colored. *Theba pisana* shells (Fig. 2B) are smaller (12–25 mm) and have a narrow umbilicus, straight peristome, and rounded aperture (Bragado et al., 2009).

Analytical samples of five to seven gastropod shells were taken from each sampled level, with the exception of BEN-1 and TOR-1 in which eleven and nine specimens were selected for AAR dating, respectively. The shells were carefully sonicated and cleaned with water to remove sediment in the laboratory. Peripheral parts, ~20–30%, were removed after chemical cleaning of the sample with 2 M hydrochloric acid (HCl). For all the specimens, we took a small sample near the aperture, a procedure reported to reduce variability within the overall sample (Murray-Wallace, 1995). We subjected ~5–30 mg of sample to AAR analysis to determine the total amino acid content. The sample preparation protocol involved hydrolysis, which was performed in a nitrogen atmosphere in HCl for 20 h at 100°C, following the methods of Goodfriend (1991) and Goodfriend and Meyer (1991) to be able to compare AAR/epimerization ratios determined previously in the Biomolecular Stratigraphy Laboratory (e.g., Torres et al., 1997). Amino acid concentrations and racemization/epimerization ratios were quantified using high performance liquid chromatography (HPLC), following the protocol described in Kaufman and Manley (1998) and Kaufman (2000): the

https://doi.org/10.1017/qua.2018.128 Published online by Cambridge University Press

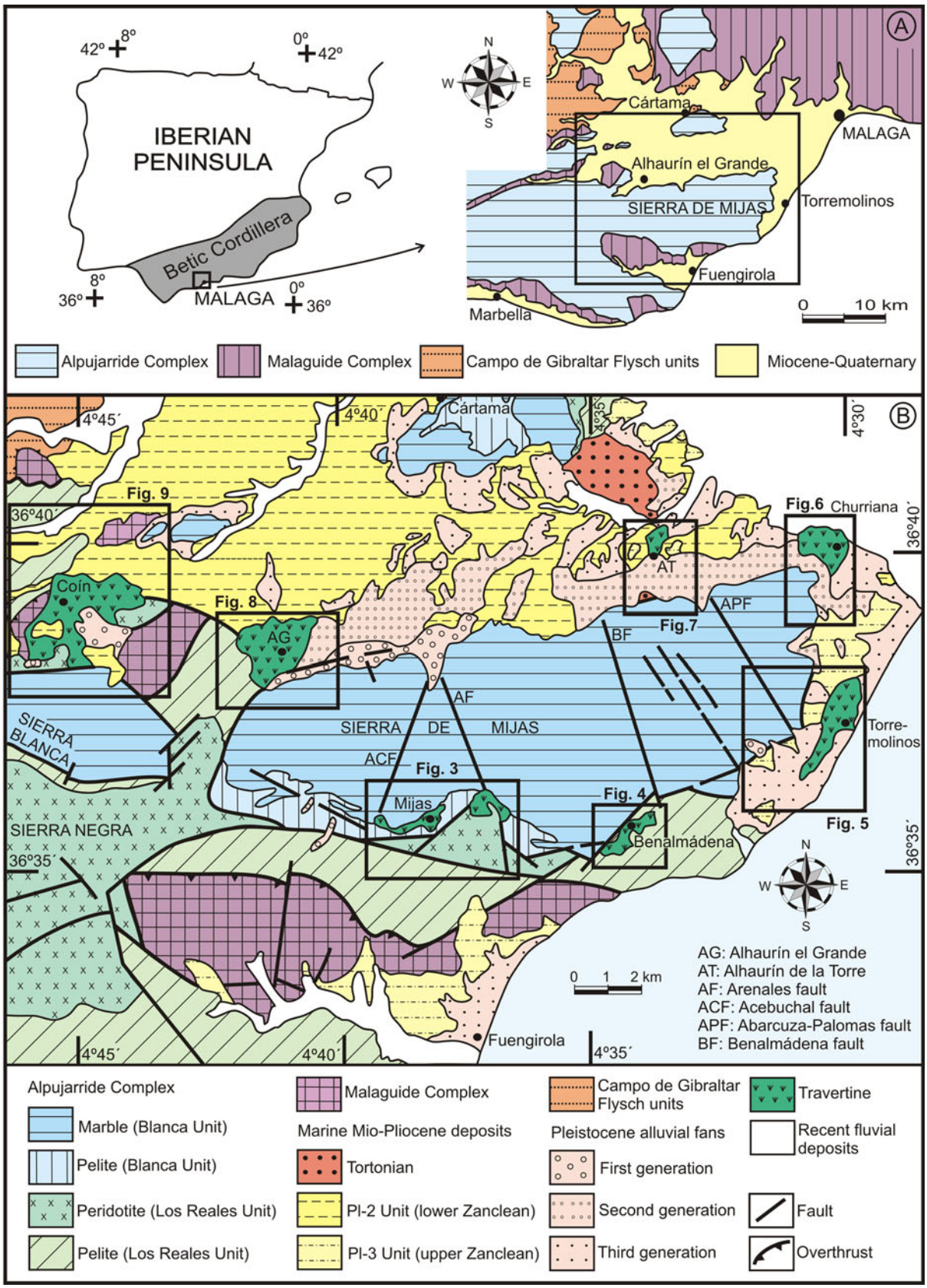


**Figure 1.** (A) Location of the Sierra de Mijas in the geologic context of the Internal Zone of the Betic Cordillera. (B) Geologic map of the Sierra de Mijas and its surroundings, showing the main outcrops of the travertine buildups. (For interpretation of the references to color in this figure legend, the reader is referred to the web version of this article.)

https://doi.org/10.1017/qua.2018.128 Published online by Cambridge University Press

**Table 1.** Age of the travertines studied from the method of amino acid racemization in samples of Helicidae gastropods. Allo: alloisoleiucine; Ile: isoleucine; Leu: leucine; Asp: aspartic acid; Phe: phenylalanine; Glu: glutamic acid.

| Samples | N | Species | D-allo/L-Ile | D/L Leu | D/L Asp | D/L Phe | D/L Glu | Age (ka) |
|---|---|---|---|---|---|---|---|---|
| MIJ-1 | 5 | *Otala punctata* | 0.179 ± 0.031 | 0.278 ± 0.039 | 0.433 ± 0.043 | 0.413 ± 0.045 | 0.202 ± 0.025 | 52.6 ± 12.4 |
| MIJ-2 | 6 | *Otala punctata* | 0.085 ± 0.029 | 0.140 ± 0.019 | 0.328 ± 0.053 | 0.201 ± 0.056 | 0.141 ± 0.022 | 28.9 ± 10.2 |
| MIJ-3 | 5 | *Otala punctata* | 0.076 | 0.224 | 0.368 | 0.264 | 0.194 | 40.3 ± 13.1 |
| MIJ-5 | 5 | *Otala punctata* | 0.084 ± 0.025 | 0.131 ± 0.018 | 0.329 ± 0.015 | 0.186 ± 0.031 | 0.111 ± 0.014 | 24.5 ± 2.4 |
| MIJ-6 | 5 | *Otala punctata* | 0.074 ± 0.034 | 0.114 ± 0.043 | 0.254 ± 0.064 | 0.128 ± 0.102 | 0.124 ± 0.033 | 22.6 ± 11.0 |
| MIJ-7 | 5 | *Otala punctata* | 0.021 ± 0.020 | 0.045 ± 0.009 | 0.138 ± 0.044 | 0.065 ± 0.033 | 0.061 ± 0.015 | 7.9 ± 7.2 |
| BEN-1 | 11 | *Otala punctata* | 0.186 ± 0.059 | 0.192 ± 0.045 | 0.262 ± 0.057 | 0.126 ± 0.043 | 0.224 ± 0.044 | 43.1 ± 16.2 |
| TOR-1 | 7 | *Otala punctata* | 0.345 ± 0.037 | 0.440 ± 0.027 | 0.476 ± 0.049 | 0.430 ± 0.055 | 0.456 ± 0.084 | 113.7 ± 52.7 |
| TOR-2 | 6 | *Otala punctata* | 0.147 ± 0.015 | 0.211 ± 0.041 | 0.420 ± 0.043 | 0.320 ± 0.068 | 0.188 ± 0.021 | 35.5 ± 6.7 |
| TOR-3 | 5 | *Otala punctata* | 0.186 ± 0.044 | 0.224 ± 0.040 | 0.426 ± 0.023 | 0.351 ± 0.129 | 0.198 ± 0.047 | 64.6 ± 25.3 |
| CHU-1 | 6 | *Otala punctata* | 0.363 ± 0.065 | 0.440 ± 0.046 | 0.426 ± 0.044 | 0.510 ± 0.082 | 0.309 ± 0.025 | 88.0 ± 28.2 |
| CHU-2 | 5 | *Theba pisana* | 0.069 ± 0.015 | 0.033 ± 0.007 | 0.136 ± 0.022 | 0.065 ± 0.024 | 0.054 ± 0.013 | 6.4 ± 6.4 |
| CHU-4 | 5 | *Otala punctata* | 0.273 ± 0.047 | 0.216 ± 0.030 | 0.406 ± 0.053 | 0.320 ± 0.062 | 0.167 ± 0.053 | 42.8 ± 18.3 |
| CHU-5 | 7 | *Otala punctata* | 0.163 ± 0.056 | 0.176 ± 0.041 | 0.349 ± 0.033 | 0.202 ± 0.047 | 0.137 ± 0.013 | 28.8 ± 8.5 |
| ALH-2 | 6 | *Otala punctata* | 0.122 ± 0.020 | 0.226 ± 0.043 | 0.416 ± 0.043 | 0.333 ± 0.034 | 0.167 ± 0.029 | 42.3 ± 14.0 |
| ALH-3 | 6 | *Theba pisana* | 0.050 ± 0.017 | 0.035 ± 0.004 | 0.179 ± 0.009 | 0.049 ± 0.007 | 0.056 ± 0.007 | 7.2 ± 3.9 |
| COI-1 | 5 | *Otala punctata* | 0.077 ± 0.019 | 0.119 ± 0.028 | 0.276 ± 0.074 | 0.185 ± 0.037 | 0.189 ± 0.023 | 36.9 ± 16.7 |
| COI-2 | 6 | *Theba pisana* | 0.093 ± 0.023 | 0.141 ± 0.019 | 0.278 ± 0.018 | 0.155 ± 0.032 | 0.116 ± 0.015 | 20.3 ± 5.5 |
| COI-3 | 5 | *Theba pisana* | 0.083 ± 0.021 | 0.074 ± 0.050 | 0.183 ± 0.045 | 0.153 ± 0.058 | 0.128 ± 0.004 | 13.4 ± 14.4 |
| COI-4 | 5 | *Otala punctata* | 0.081 ± 0.051 | 0.056 ± 0.018 | 0.209 ± 0.059 | 0.101 ± 0.063 | 0.069 ± 0.023 | 11.6 ± 6.3 |

hydrolysates were evaporated to dryness *in vacuo* and then rehydrated in 10 µL/mg of 0.01 M HCl with 1.5 mM sodium azide and 0.03 mM L-homo-arginine (internal standard). Samples were injected into an Agilent HPLC-1100 equipped with a fluorescence detector. Excitation and emission wavelengths were programmed at 230 and 445 nm, respectively. A Hypersil BDS C18 reverse-phase column (5 µm; 250 x 4 mm i.d.) was used for the analysis.

Derivatization was undertaken before injection by mixing the sample (2 µl) with the pre-column derivatization reagent (2.2 µl), which was composed of 260 mM isobutyryl-L-cysteine (chiral thiol) and 170 mM o-phthaldialdehyde, dissolved in a 1.0 M potassium borate buffer solution at pH 10.4. Analytical conditions are presented in Table S1-Supplementaty Information. We separated the D and L peaks of the following amino acids: aspartic acid and asparagine (Asx), glutamic acid and glutamine (Glx), serine (Ser), alanine (Ala), valine (Val), phenylalanine (Phe), isoleucine (Ile), leucine (Leu), threonine (Thr), arginine (Arg), tyrosine (Tyr), and glycine (Gly).

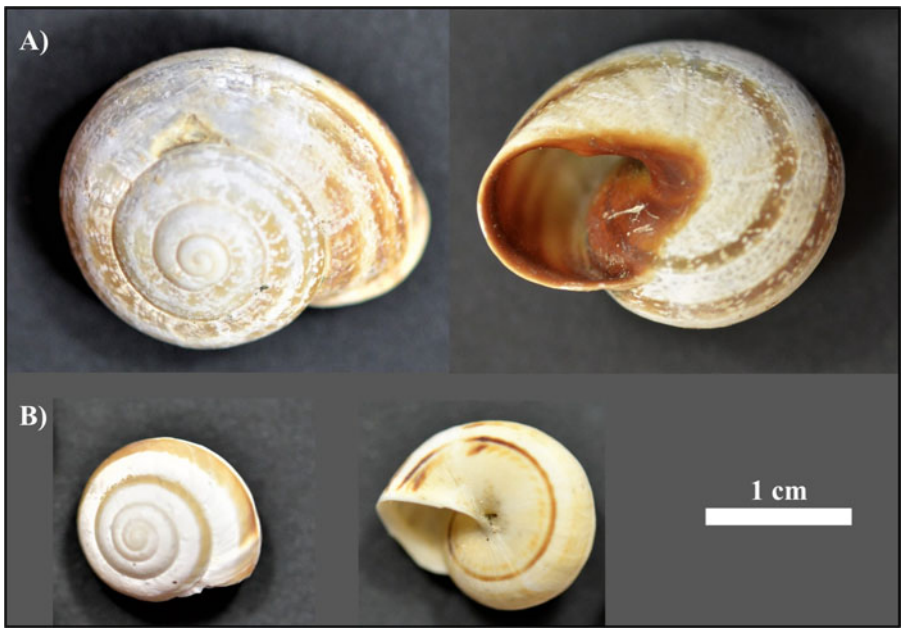


**Figure 2.** (color online) Land snail shells from Costa del Sol travertine deposits. (A) *Otala punctata* from CHU-1. (B) *Theba pisana* from TOR-2.

https://doi.org/10.1017/qua.2018.128 Published online by Cambridge University Press

## AAR dating of the travertines

A total of 118 samples taken from the aperture of Helicidae shells were analyzed for amino acid content. Of these, 32 results (25.4% of the data: 1 in MIJ-2, 4 in MIJ-3, 2 in MIJ-6, 7 in BEN-1, 6 in TOR-1, 1 in TOR-2, 2 in TOR-3, 2 in CHU-5, 1 in ALH-2, 1 in ALH-3, 1 in COI-1, 2 in COI-2, and 2 in COI-3) were excluded due to their low amino acid content, because their D/L values of different amino acids fell off the covariance trend (cf. Kaufman, 2003, 2006; Laabs and Kaufman, 2003), and/or because of abnormally high/low racemization/epimerization values, characterized by D/L values falling outside the 2σ range of the group (cf. Hearty et al., 2004; Kosnik and Kaufman, 2008) (Table S2-Supplementaty Information). We did not include outliers for the age calculation of the different travertine levels.

According to Goodfriend (1991), the analysis of more than one amino acid provides largely redundant information on sample age. Thus, to establish the aminochronology of the travertine deposits, we used the Ile, Leu, Asp, Phe, and Glu contents of Helicidae shells. The mean Asp, Glu, Leu, Ile, and Phe D/L values in each travertine level are shown in Table 1 together with their ages. The numerical age of each level was calculated by introducing the Asp, Glu, Leu, Ile, and Phe D/L values determined in the gastropod shells of that level into the age-calculation algorithms established by Torres et al. (1997) for gastropods in the central and southern part of the Iberian Peninsula. The age uncertainty is the standard deviation of all the values obtained from these amino acids (Ile, Leu, Asp, Phe, and Glu) in the 5–11 specimens analyzed in each level.

There are two potential issues that challenge the validity of our AAR ages. First, although monogeneric samples are necessary to reduce taxonomically-controlled variability in D/L values (Penkman et al., 2007, 2008; Ortiz et al., 2013), we employed two different gastropod taxa to establish the ages of the travertine deposits of the Costa del Sol area. Since the analyzed land snails here belong to the same family (Helicidae), we used the algorithms of Torres et al. (1997) to calculate the ages. In fact, according to Torres et al. (1995, 1999), the AAR kinetics of Helicidae specimens could be assimilated to this model; differences in racemization ratios of species diminish with increasing age. Therefore, ages obtained in gastropods from this study using the equations of Torres et al. (1997) were reliable. Moreover, it must be highlighted that our intention was to date the units at the scale of MIS since it is difficult to identify substages due to time-averaging and post-depositional processes.

AAR is a temperature-dependent process and therefore age-calculation algorithms can be established only from samples located in areas with the same thermal history. The algorithms that Torres et al. (1997) obtained for land snails from central and southern Spain (where the Costa del Sol is located) have similar current mean annual temperatures (Rivas-Martínez and Rivas-Sáenz, 2009). Moreover, these areas followed the same glacial-interglacial cycles since they belong to the Mediterranean climatic region (Rubel and Kottek, 2010; Chen and Chen, 2013) and show the same paleoenvironmental variations as those obtained by Sánchez-Goñi et al. (1999, 2002, 2008) for the late Quaternary.

In general, the uncertainties associated with AAR ages (obtained using 5–11 analytical samples) were higher than those usually obtained with other dating methods such as radiocarbon dating. Generally, ages obtained by other methods are performed using a single sample, and the uncertainties are attributed only to the sample error. However, when a number of analytical samples from the same horizon are dated using $^{14}C$, then the differences are larger. Thus, a relatively high uncertainty for the age of the samples can be explained if we use different amino acids (Asp, Glu, Leu, Ile, and Phe) and diverse samples (5–11) for the age calculation of a particular level.

In any case, the reliability of the AAR ages obtained in our study was confirmed by the comparison with the numerical ages provided by Durán (1996) and Durán et al. (1988) in the same travertine deposits with other dating methods, such as U/Th and ESR (see Discussion and Fig. 11).

## Buildup and chronometric data for the travertines

### *Travertines of the Mijas sector*

In the Mijas sector, various travertine masses with different altitude, outcrop surface, thickness, and cementation degree unconformably lie on marble, gneiss, and peridotite of the Alpujarride Complex (Fig. 3A). The town of Mijas and the sanctuary of San Antón are built onto the two largest, highest (400–300 m asl), and most cemented travertine bodies. Both these travertines constitute platforms with proximal and distal carbonate facies. Proximal facies are mainly composed of facies that were bioconstructed by higher plants with abundant tubes in a subhorizontally bedded array, and subsidiarily, calcareous accretions and botryoidal stromatolite growths. In the distal position, nearly vertical beds formed of large stems and stromatolite crusts constitute a cascade facies. Most distally, beds dipping 15–30° downslope are also mainly composed of bioconstructed facies frequently made of vertical but also inclined or horizontal tubular remains of plants characterizing a slope zone. Locally, these travertines overlie basal conglomerate or breccia. This platform-cascade-slope set represents the first stage of travertine development in the Mijas area and is identified as TM-1.

TM-1 was eroded by the incision of a gully and was afterwards filled by 4–6 m of travertine and detrital deposits containing gastropods in the westernmost part of the outcrop of Mijas (Fig. 3B) and to the east of the San Antón sanctuary (Fig. 3C). The travertine beds were made up of bioconstructed facies with abundant tubes and leaves and by oncolitic gravels. These beds are exposed at a lower altitude (350–380 m) and represent a travertine of fluvial type facies (hereafter TM-2) younger than those represented by the upper platform (TM-1).

https://doi.org/10.1017/qua.2018.128 Published online by Cambridge University Press

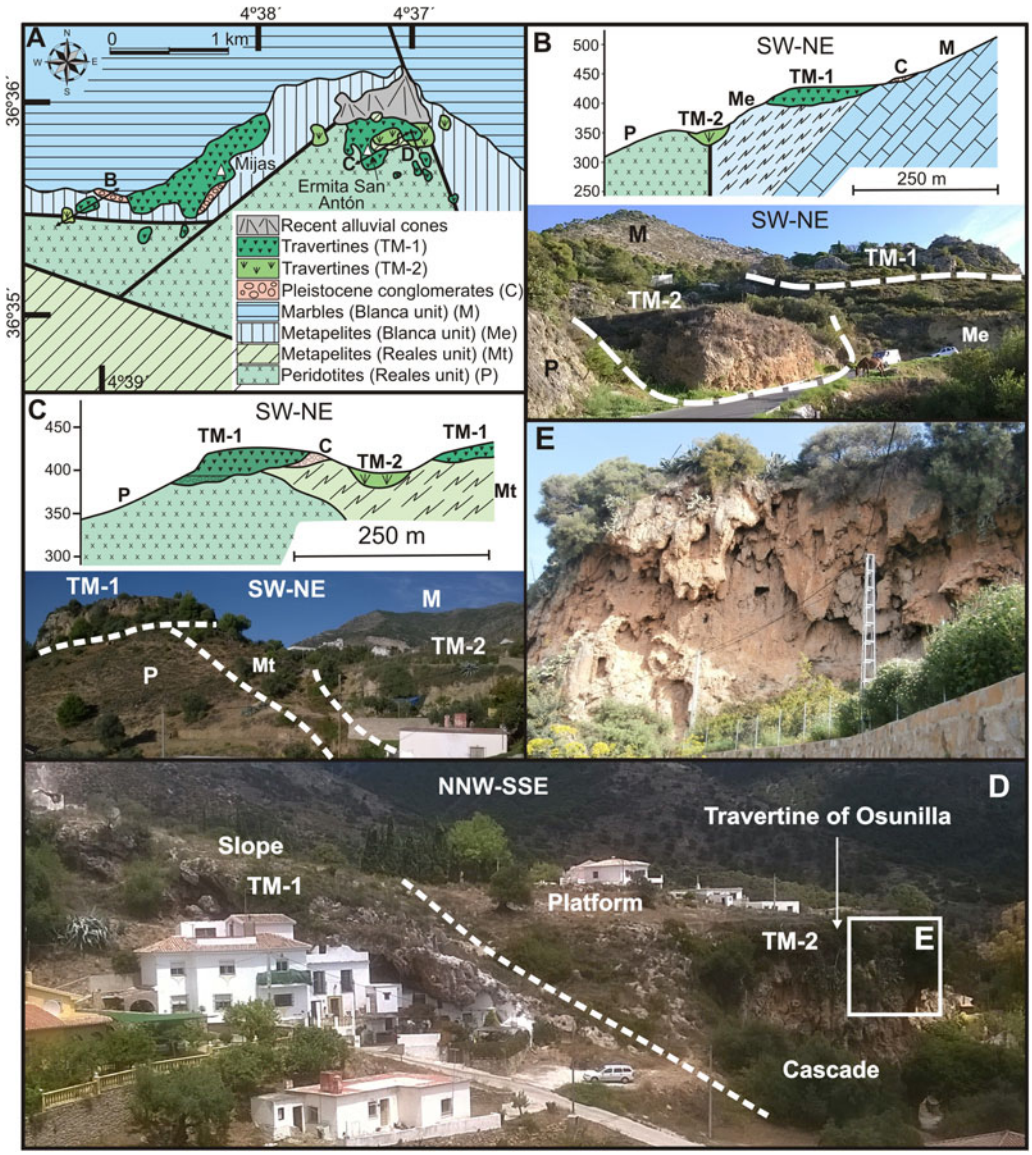


**Figure 3.** (color online) (A) Geological map and location of travertines in the Mijas sector. (B) Cross-section and view differentiating the two stages of travertine growth in the westernmost part of the outcrop of Mijas. (C) Cross-section and view differentiating the two stages of travertine growth to the east of the San Antón sanctuary. (D) The travertine of Osunilla (TM-2) developed over the slope facies of the upper platform (TM-1). (E) Cascade facies of the travertine of Osunilla (TM-2).

The AAR chronologic results from gastropods yield an age of 52.6 ± 12.4 ka for the TM-2 to the west of the town of Mijas (sample MIJ-1 in Table 1). Three ages (from below to above, samples MIJ-6, MIJ-2, and MIJ-5 in Table 1) indicate that growth would have taken place between 28.9 ± 10.2 and 22.6 ± 11.0 ka for the TM-2 of the sanctuary of San Antón. Furthermore, in these travertines, cavities were filled with clay and uncemented travertine remains with gastropods dating to 7.9 ± 7.2 ka (sample MIJ-7 in Table 1).

Another small travertine mass (identified as "Travertine of Osunilla," Fig. 3D) appears at 360–390 m asl embedded in the slope facies of the upper platform (TM-1) just to the east of the San Antón sanctuary outcrop. The lower part of the travertine of Osunilla is made of 2 m of travertine fragments in a clayed matrix containing gastropods that yield an age of 40.3 ± 13.1 ka (sample MIJ-3 in Table 1). Above this, levels are 10–15 m of bioconstructed travertine facies with abundant vertical arranged tubes (Fig. 3E) characterizing the cascade facies. Based on the age and topographical height, the travertine of Osunilla is also associated with episode TM-2.

### *Travertines of the Benalmádena sector*

The different travertine masses in the Benalmádena sector overlie pelite of the Los Reales Unit, close to the fault contact with the marble of the Blanca Unit (Fig. 4A). Two stages of travertine development are identified based on differences in altitude, degree of cementation, and AAR ages.

Travertines belonging to the older stage (TB-1) are located at 190–250 m asl and are strongly cemented (Fig. 4B and C). This cluster represents a platform composed

https://doi.org/10.1017/qua.2018.128 Published online by Cambridge University Press

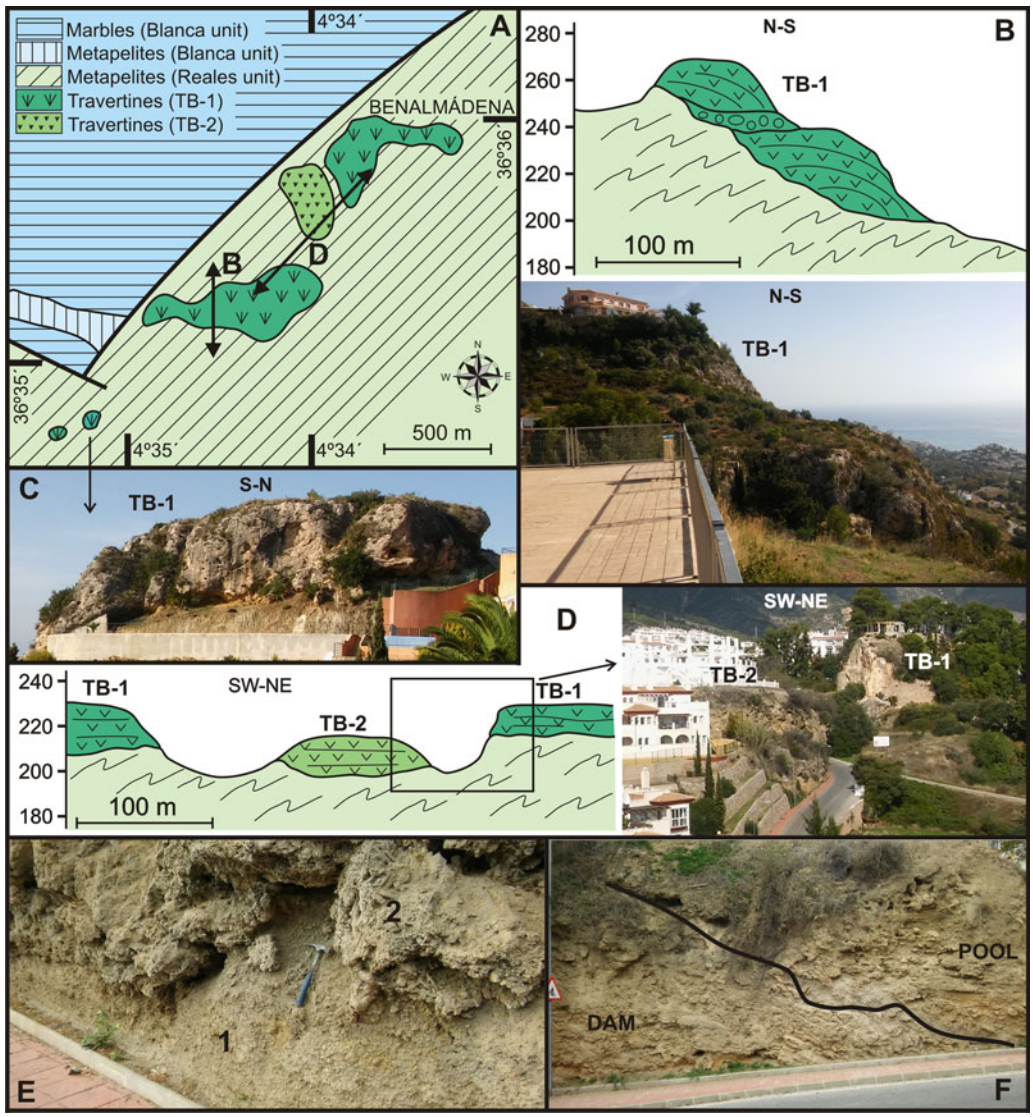


**Figure 4.** (color online) (A) Geological map and location of travertines in the Benalmádena sector. (B) Cross-section and photography showing the platform-cascade system of the TB-1 travertine. (C) Slope facies of the TB-1 travertine. (D) Cross-section and view differentiating the two stages of travertine growth in the Benalmádena sector. (E) Oncolitic facies (1) and bioconstructed facies of small stems (2) of the TB-2 travertine. (F) Pool-dam system in the TB-2 travertine.

of bioconstructed facies composed mainly of small stems of plants. In its distal part, quite vertical walls are preserved with the remains of large stems and stromatolite growths representing a cascade area. At the bottom, reworked blocks of travertine are scattered in a slope zone. The two small exposures located farther to the southwest (Fig. 4A and C) are made up of travertine facies bioconstructed by small stems of plants that have stratification dipping towards the slope and that represent distal facies within the slope. No gastropods were found in this travertine, but two available ESR ages of 86.3 ± 17 and 109.0 ± 22 ka were obtained by Durán et al. (1988).

The second travertine stage (TB-2) consists of poorly-cemented facies appearing at a lower altitude (< 200–230 m asl) in a gully carved in the older travertine platform (Fig. 4A and D). The lower part of the TB-2 travertine is made of 2 m of oncolitic detrital facies with abundant fragments of small stems and occasionally boulders of marble and schist (1 in Fig. 4E). These facies gently dip downslope and, above an irregular contact, they are covered by 10–12 m of bioconstructed facies of small stems, having high porosity and faint horizontal stratification (2 in Fig. 4E). These latter facies represent a barrier zone formed in the gully, leading to the development of a depressed area upstream where oncolitic facies with horizontal stratification were deposited (Fig. 4F). Gastropods collected from the oncolitic travertine facies of the TB-2 date to 43.1 ± 16.2 ka (sample BEN-1 in Table 1).

### *Travertine of Torremolinos*

The travertine of Torremolinos overlies lower Pliocene marine deposits of the PL-3 unit (Guerra-Merchán et al., 2000, 2014) and change laterally westward to Pleistocene

https://doi.org/10.1017/qua.2018.128 Published online by Cambridge University Press

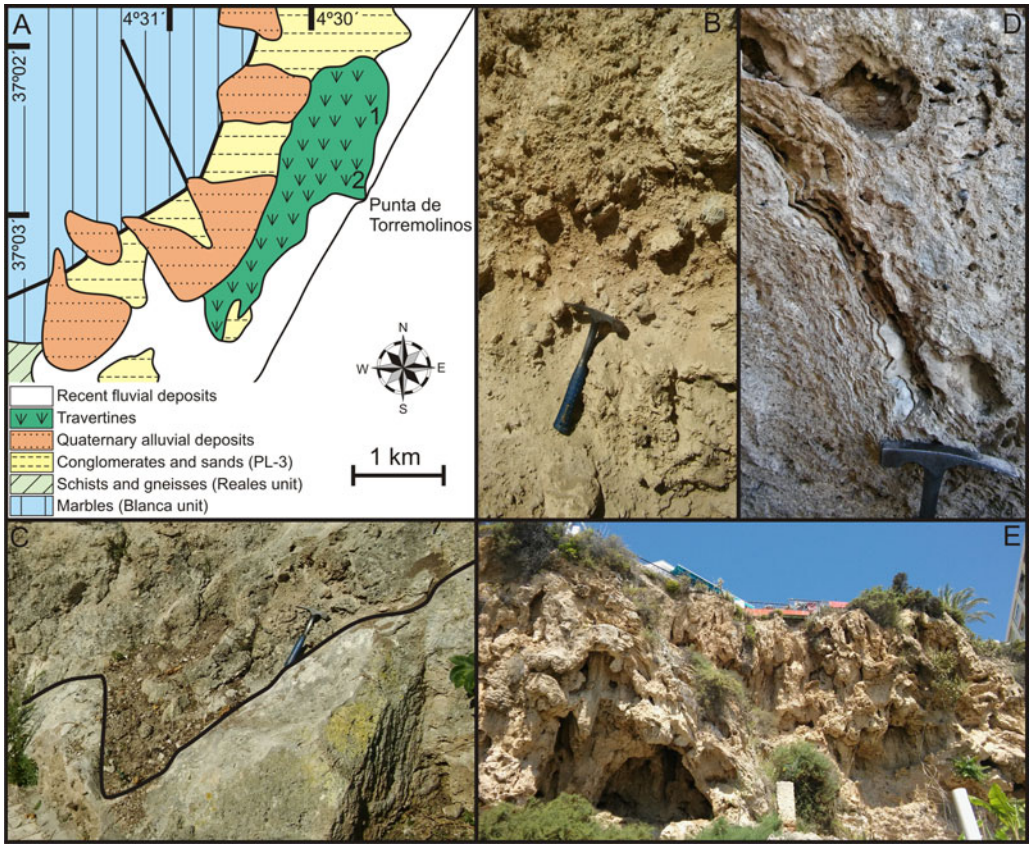


**Figure 5.** (color online) (A) Geological map and location of travertines in the Torremolinos sector. (B) Cascade-foot or slope deposits in site 1 of the "Las Mercedes" street. (C) Encrusted erosional surface in site 1. (D) Thin layers of stromatolite facies with steep inclination in site 1. (E) Cascade area in site 2 ("Punta de Torremolinos").

alluvial deposits (Fig. 5A). The upper surface of this travertine is almost completely urbanized and its features can be studied only in the northern part and near the coast in vertical exposures (sites 1 and 2 in Fig. 5A). In site 1 ("Las Mercedes" street), the lower part consists of 2–3 m of travertine fragments of varying sizes (Fig. 5B) in poorly-stratified beds with encrusted surfaces (Fig. 5C), suggesting cascade-foot or slope deposits. Above the basal travertine fragments overlie 13–15 m of bioconstructed facies, generally of large vertical stems and locally with abundant leaves, among which frequent stromatolite and botryoidal growths are visible in the thin layers with steep inclination (Fig. 5D). These latter facies seem to represent the barrier and cascade area, which progress over the lower facies.

Two facies associations are recognized at site 2 (Punta de Torremolinos; Fig. 5A). In the proximal part, horizontally-bedded oncolitic facies alternate with facies bioconstructed by small stems that had formed in a pool, whereas in distal position, bioconstructed facies made of lager stems alternating with stromatolite crusts growing on vertical surfaces would represent the cascade area, in which large cavities are frequently found (Fig. 5E).

The AAR data on gastropods provide different ages. In site 1, the AAR age of 113.7 ± 52.7 ka (sample TOR-1 in Table 1) has a large uncertainty associated with it because of the low available quantity of amino acids. At this same site, one gastropod collected from the fill of a cavity yielded an age of 35.5 ± 6.7 ka (sample TOR-2 in Table 1). Gastropods from the upper part of the outcrop of Punta de Torremolinos were dated to 64.6 ± 25.3 ka (sample TOR-3 in Table 1). These contrasting ages suggest that the travertine of Torremolinos is polyphasic, but the outcrop conditions do not allow distinguishing significant features indicative of the different phases.

### *Travertines of the Churriana sector*

Three travertine masses are recognized in the vicinity of Churriana. One of the largest travertine masses is located within the town itself, and another two masses located ~2 km south of the town are very small (Fig. 6A). Several stages of travertine growth can be differentiated from the types of facies, the degree of cementation, and the chronology.

The oldest travertine deposit in the Churriana area (TCH-1) is located close to the foothill of Sierra de Mijas. This travertine overlies lower Pliocene marine deposits (site 1 in Fig. 6A) and was dated by Durán (1996) to >350 ka. The travertine is relatively well cemented, encrusted on its top, and does not contain any gastropods; hence it was not possible to date with AAR methods.

https://doi.org/10.1017/qua.2018.128 Published online by Cambridge University Press

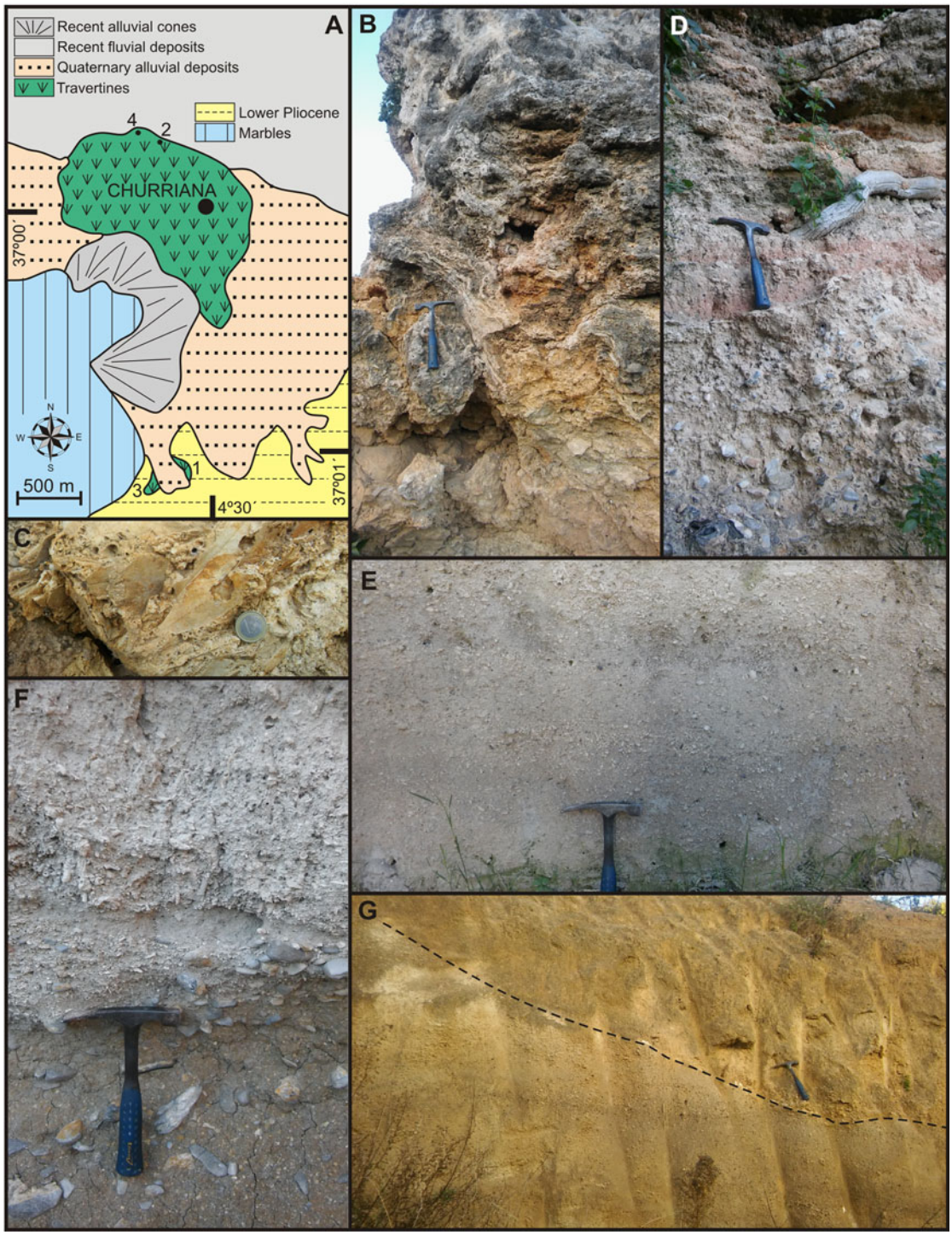


**Figure 6.** (color online) (A) Geological map and location of travertines in the Churriana sector. (B) Dam and cascade facies in the TCH-1 travertine. (C) Remains of leaves in the dam facies of the TCH-1 travertine. (D) Alternation of clastic and travertine layers deposited in the pool of the TCH-1 travertine. (E) Facies of oncolitic calcirudites in the TCH-2 travertine. (F) Detrital deposits covered by a bed made of fragmented stems and oncolites in the TCH-3 travertine. (G) Erosional surface separating the travertine masses of the TCH-2 and TCH-4 stages.

Travertine facies bioconstructed by large and small stems and leaves, intercalating stromatolite growths on tilted surfaces, predominate in the most distal part (eastwards and farther from the relief of the sierra) (Fig. 6B and C). These facies characterize an area of dam and cascade. In the proximal position (Fig. 6D), the base is made up of a cemented breccia made of marble boulders and travertine fragments (1–1.5 m thick) and changes upwards to 2 m of calcirudites with intercalations of facies bioconstructed by stems and stromatolite growths. The stromatolite facies could represent the pool area.

The main travertine mass, on which the town of Churriana is built, belongs to a second stage (TCH-2). There is a lack of

https://doi.org/10.1017/qua.2018.128 Published online by Cambridge University Press

exposures in this travertine deposit due to buildings and farmland. Oncolitic calcirudites facies with gastropods predominate in this travertine, which is 10–15 m thick and has faint horizontal stratification linked to the variation in the size of the oncolites (Fig. 6E). Laterally, lenticular bioconstructed facies of stems in life position seem to represent travertine growth in a lagoonal environment. Locally, cm-thick stromatolite growths that dip 30–40° indicate the local development of small dams and cascades. Gastropods sampled from the oncolitic facies in the northern area of this outcrop (site 2 in Fig. 6A) yield an AAR age of 88.0 ± 28.2 ka (sample CHU-1 in Table 1).

A small travertine mass that crops out to the south of Churriana (site 3 in Fig. 6A) seems to have originated in a third stage (TCH-3). Some 4–5 m thick, the travertine is composed of an alternation of detrital deposits and travertine beds made of broken stems and oncolites with gastropods resting on a basal conglomerate deposited by debris flow processes (Fig. 6F). Gastropods from two different levels provide ages of 42.8 ± 18.0 (sample CHU-4) and 28.8 ± 8.5 ka (sample CHU-5) (Table 1).

A small travertine deposit attached to the main one (site 4 in Fig. 6A) represents a fourth stage of travertine growth (TCH-4). This small travertine deposit is separated from the previous one (TCH-2) by an erosive surface with remains of a thin, white carbonate crust (Fig. 6G) that is onlapped by orangish travertine deposits. These orangish travertine deposits are made of oncolitic calcirudites in a fining-upward sequence with locally-channeled bases. Gastropods within the travertine yield an age of 6.4 ± 6.4 ka (sample CHU-2 in Table 1), showing that it is clearly younger than that of the main stage TCH-2.

### *Travertine of Alhaurín de la Torre*

The town of Alhaurín de la Torre lies on a travertine mass, largely covered by houses, while northwards the formation is terraced for crops. The most visible outcrops are located on the western edge (1 in Fig. 7A), where 15–20 m thick of detrital facies (conglomerates and sands) alternate with travertine facies (Fig. 7D). The travertine levels, some with a lenticular shape, are composed of strongly-cemented facies bioconstructed by small stems. Northwards, in a distal position, the detrital facies change to light-colored cemented sands and the travertine levels are characterized by facies that were bioconstructed by small stems and oncolites in its lower part.

The travertine of Alhaurín de la Torre overlies lower Pliocene marine deposits (units Pl-2 and Pl-3), and towards the Sierra de Mijas the deposits lateral grade into alluvial deposits (Fig. 7B). The main travertine deposit did not yield gastropods, but they are present within the clay filling of cracks and cavities (site 2 in Fig. 7A and C), yielding age estimates of 42.3 ± 14.0 (sample ALH-2) and 7.2 ± 3.9 ka (sample ALH-3). These ages provide minimum temporal constraints on the deposition of travertines at Alhaurín del la Torre.

### *Travertine of Alhaurín el Grande*

The town of Alhaurín el Grande is also built onto a travertine deposit and is terraced. This travertine deposit rests on Alpujarride gneiss and schist, Pliocene marine deposit, and Pleistocene alluvial deposit, but it is not in direct contact with the marble of the Sierra de Mijas (Fig. 8A).

Two facies associations change laterally from one to the other near the cemetery at Alhaurín el Grande (Fig. 8B). In a proximal position, the sequence has horizontal beds with oncolitic facies at the bottom (6–7 m thick), while upwards of 15 m thick of alternations of oncolites and bioconstructions of small stems appear (Fig. 8C). This association suggests a travertine growth in a pool area. In the distal position, stem bioconstructed facies predominate, in which small cavities appear as well as surfaces covered by unspecified botryoidal growths (Fig. 8D and E). This arrangement would correspond to the barrier zone of the pool. No gastropods were found in the travertine and thus it was not possible to date this deposit with AAR methods. Durán (1996), however, obtained a single U/Th age of $28.7^{+3.0}/_{-2.8}$ ka for this travertine.

### *Travertines of the Coín sector*

Travertines in the environs of the town of Coín (Fig. 1B) are related to springs from the small Sierra Blanca de Coín, which are developed on a metamorphic basement and lower Pliocene marls and sands (unit Pl-2; Guerra-Merchán et al., 2000, 2014). Two travertines are recognized at different heights in this sector (Fig. 9A and B). The highest travertine (TC-1) is located in the hills south of Coín between 300 and 330 m asl. TC-1 consists of small, strongly-cemented masses in which the cementation does not allow clear recognition of the facies and is devoid of gastropods. Considering that no previous datings are available, age control of this unit is lacking.

The main travertine deposits (TC-2) occupy a broad expanse around Coín at 250–290 m asl (Fig. 9A and B) and have a stepped morphology, where several platforms at different heights are limited by escarpments (Fig. 9A and C). Horizontal beds of fine-grained carbonate facies containing ovoid oncolites predominate and occasionally intercalate botryoidal or cupular stromatolites are present in the platform areas (Fig. 9D and F). In minor proportion, facies bioconstructed with abundant remains of stems in varying disposition appear (Fig. 9E). In the upper part of this travertine, the layers change to calcarenites or calcilutites bearing gastropods. These platform areas would result from travertine growth in a lagoonal environment.

The escarpment areas between the platforms have steeply dipping beds composed mainly by great plant stems in life position (Fig. 9G), frequently culminated by layers of laminar stromatolites (Fig. 9H). Some beds contain reworked travertine blocks in the lower part of the escarpments (Fig. 9I). These facies seem to correspond to travertine growth in dams and cascades.

https://doi.org/10.1017/qua.2018.128 Published online by Cambridge University Press

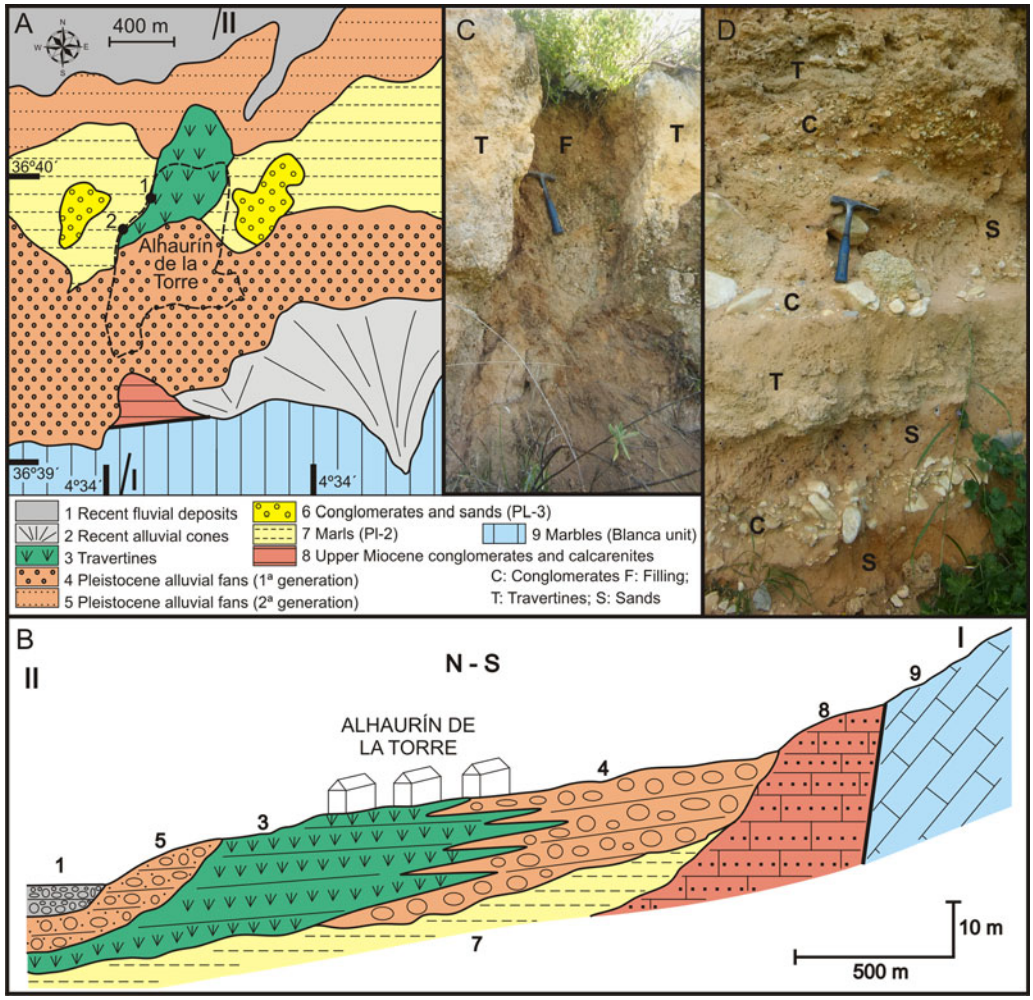


**Figure 7.** (color online) (A) Geological map and location of travertines in the Alhaurín de la Torre sector. (B) Cross-section showing the stratigraphic relationships of the travertine of Alhaurín de la Torre with the lower Pliocene marine deposits and with those of the Pleistocene alluvial. (C) Earthy material filling cracks and cavities. (D) Alternation of detrital and travertine facies.

Gastropod specimens were collected at four points (sites 1 to 4 in Fig. 9) in this travertine buildup and yield ages between 11.6 ± 6.3 and 36.9 ± 16.7 ka (samples COI-1, COI-2, COI-3, and COI-4 in Table 1).

## DISCUSSION

In the travertines studied, no evidence of hydrothermal activity was found, and thus their origin is presumably related to cold carbonate-rich waters coming from the springs of the region. Therefore, the travertines described here are meteogene travertines (Pentecost and Viles, 1994) or cool-water travertines (Ford and Pedley, 1992). Four major types of facies are recognized:

(a) facies bioconstructed by abundant remains of higher plants, usually small- and medium-sized stems, predominantly in life position. This facies is the most abundant and appears disposed in horizontal or slightly inclined dm-thick layers. The above features suggest that this facies type developed in runoff water areas or shallow pools, giving rise to platforms, dams, or slopes.

(b) facies bioconstructed by stems frequently of great size disposed in irregular, subvertical beds. This facies represents cascade areas in which synsedimentary cavities and reworked travertine blocks in the lower part appear.

(c) Oncolite facies in horizontal beds, frequently with fining-upward sequences and channeled bases, suggesting a pool depositional environment. In many cases, this facies shows an earthy matrix containing gastropod and small travertine clasts provided by inputs from the edges of the pool.

(d) botryoidal and globular stromatolite facies in beds of cm-dm thickness and variable dip, which deposited on irregular surfaces. Predominantly, this facies developed in cascade or slope areas.

Different facies associations allow recognition of three types of travertines (Fig. 10):

https://doi.org/10.1017/qua.2018.128 Published online by Cambridge University Press

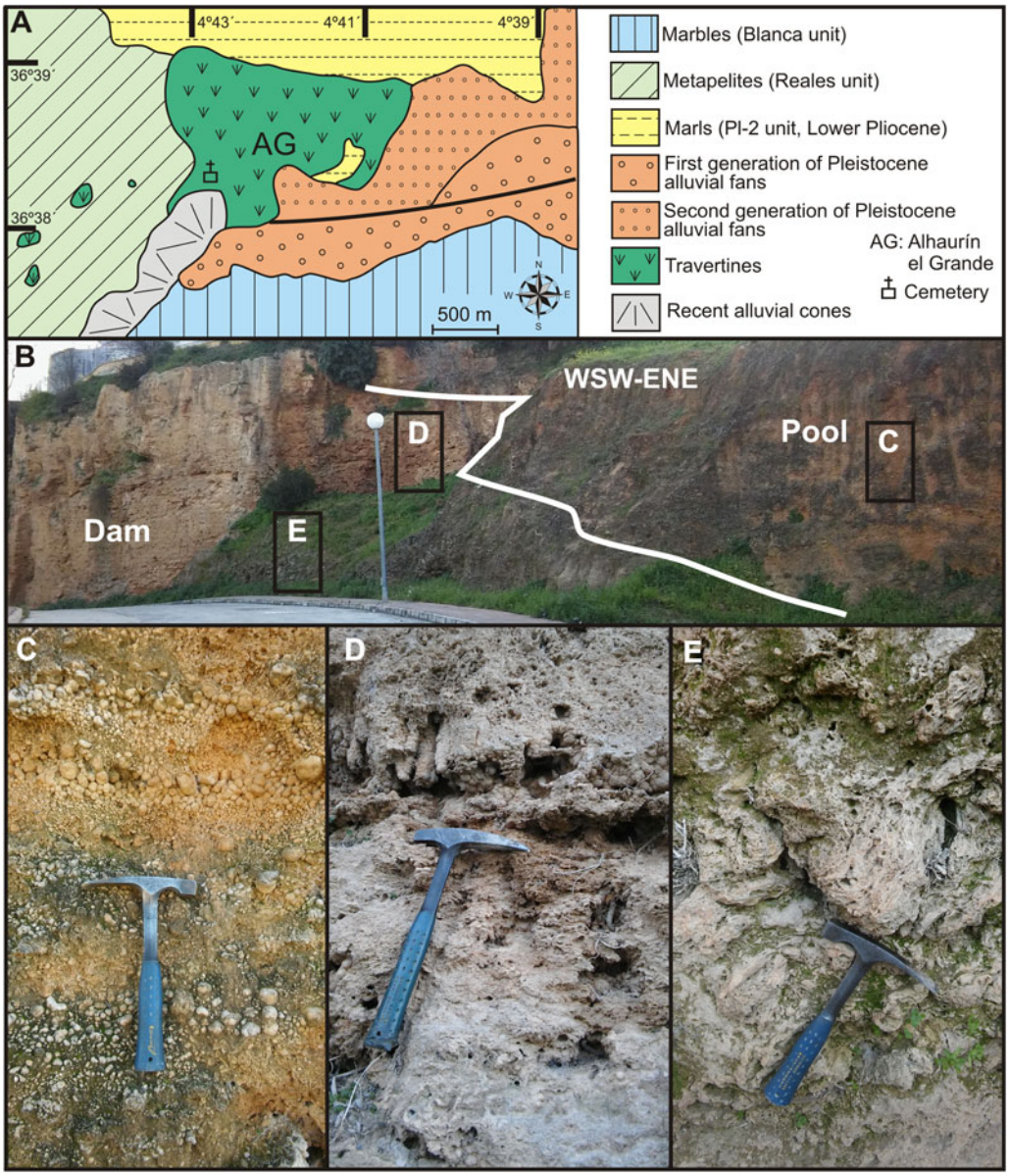


**Figure 8.** (color online) (A) Geological map and location of travertines in the Alhaurín el Grande sector. (B) View of the lateral change from pool to dam facies. (C) Horizontal beds of oncolitic facies deposited in the pool. (D) and (E) Facies bioconstructed by stems in the dam area.

(a) The first type is represented by travertine bodies in contact with carbonate basement rocks (Fig. 10A), coinciding with the position of fountainheads or springs (spring-type travertine of Magnin et al., 1991). In this case, the travertine overlies the rocky basement, although locally it could cover detrital facies deposited on a slope. After gradual spread over the surface of a slope, a platform of limited size forms and distally develops a cascade and slope system (cascade-type travertine of Pedley, 1990; Pentecost and Viles, 1994). In the study area, this type is represented in the sectors Mijas (TM-1 stage) and Benalmádena (TB-1). The travertine of Osunilla (Mijas sector, TM-2 stage) also corresponds to this type but covers the slope facies of the preceding stage (TM-1).

(b) Some small travertine buildups (Fig. 10B) appear separated from the mountainous carbonate substrate and are characterized by the alternation with detrital deposits of channel infill. These are the valley-infill model of Pedley (1990) and Pentecost and Viles (1994) or river-valley travertines of Magnin et al. (1991). The development of bioconstructed facies generates small dams where oncolitic and detrital facies are deposited. These types of travertine have been recognized in sectors of Mijas (TM-2), Benalmádena (TB-2), and Churriana (TCH-3).

(c) A third type of travertine is characterized by the development of a large platform recognizable by the predominance of well-stratified layers of oncolites and facies bioconstructed by small stems, as a result of the establishment of a pool. Frequently, they are large constructions/deposits

https://doi.org/10.1017/qua.2018.128 Published online by Cambridge University Press

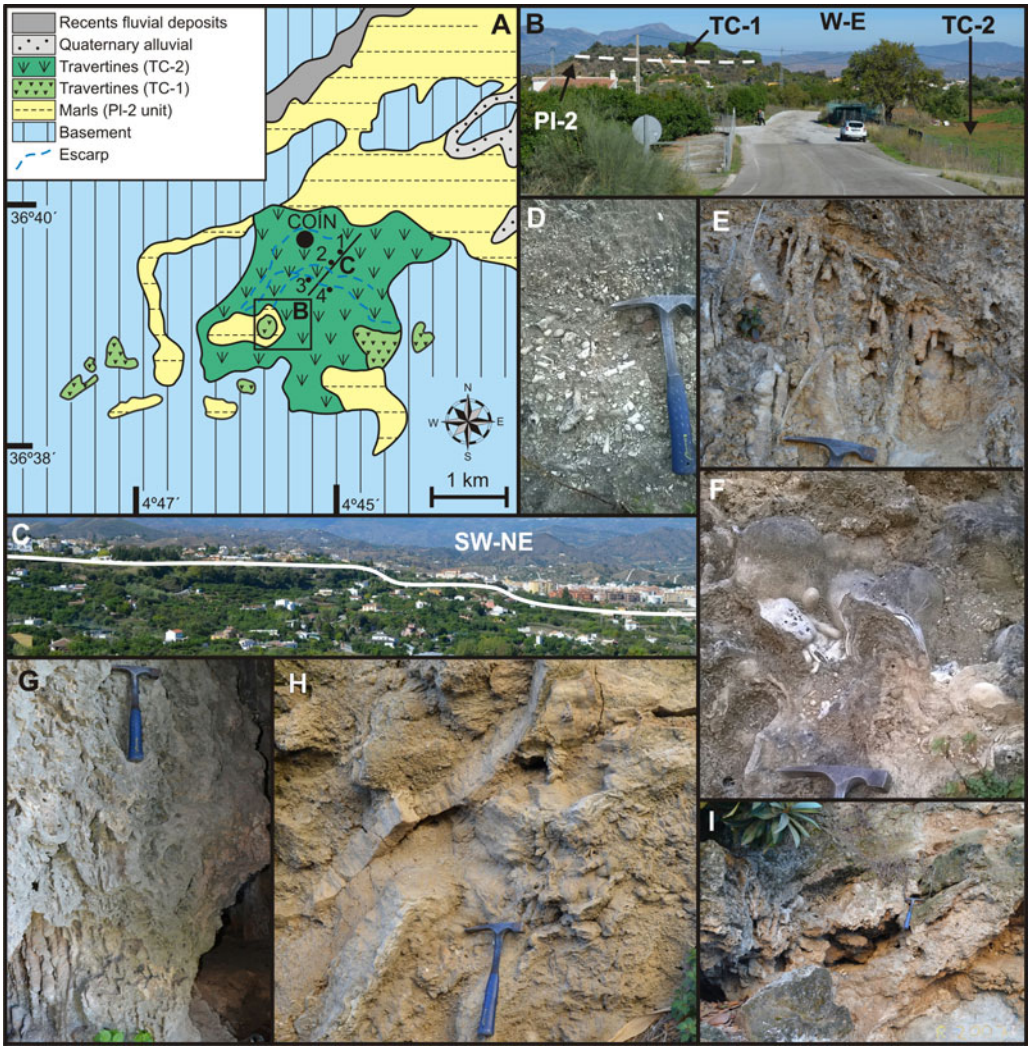


**Figure 9.** (color online) (A) Geological map and location of travertines in the Coín sector. (B) View of the development of the two travertine stages (TC-1 and TC-2) at different heights. (C) Stepped morphology of the TC-2 travertine. (D) Ovoidal oncolite facies. (E) Bioconstructed facies with abundant remains of stems. (F) Stromatolite cupolas. (G) Facies of great stems in life position. (H) Layers of laminar stromatolites. (I) Reworked travertine blocks in the lower part of one escarpment.

that grade to alluvial and fluvial deposits towards the mountain front. Distally, poorly-stratified beds mainly bioconstructed by small stems would characterize a barrier limiting the pool. Outwards they can change to steeply-dipping beds made up by large stems and stromatolite growths, so characterizing a cascade with reworked travertine blocks at its foot (Fig. 10C). This type of travertine is similar to the pool-dam-cascade model of Juliá (1983), Pedley (1990), and Ford and Pedley (1996) and is represented by the travertine buildups at Coín (TC-2), Alhaurín el Grande, Alhaurín de la Torre, Churriana (TCH-1, 2 and 4), and Torremolinos. Martín-Algarra et al. (2003) and García-García and Nieto (2005) also studied similar travertines in other sectors of the Betic Cordillera near Granada and Alcalá la Real, respectively.

Despite the high urban development and intense agricultural modifications of the landscape, the geomorphic and stratigraphical analysis and dating demonstrate that many of the travertine deposits are polyphasic. This was previously demonstrated for the travertines of Torremolinos by Durán et al. (2002). Our study demonstrates that the travertines in the Mijas, Benalmádena, Churriana, and Coín sectors also grew in several stages at different altitudes separated by erosive surfaces. The AAR ages for gastropods from the different travertines, complemented with previous dating by U/Th series and ESR (Durán et al., 1988; Durán, 1996; Durán et al., 2002), allow us to establish five significant stages of travertine development.

The oldest available age comes from the travertine of Churriana (TCH-1), where gastropods have not been found, but Durán (1996) proposed that it is younger than the early Pliocene and older than 350 ka based on field relations and U-series dating. This suggests an initial stage with significant eastward groundwater drainage from the Sierra de Mijas.

A second stage of travertine development occurred during the middle Pleistocene and is represented by the travertines at

https://doi.org/10.1017/qua.2018.128 Published online by Cambridge University Press

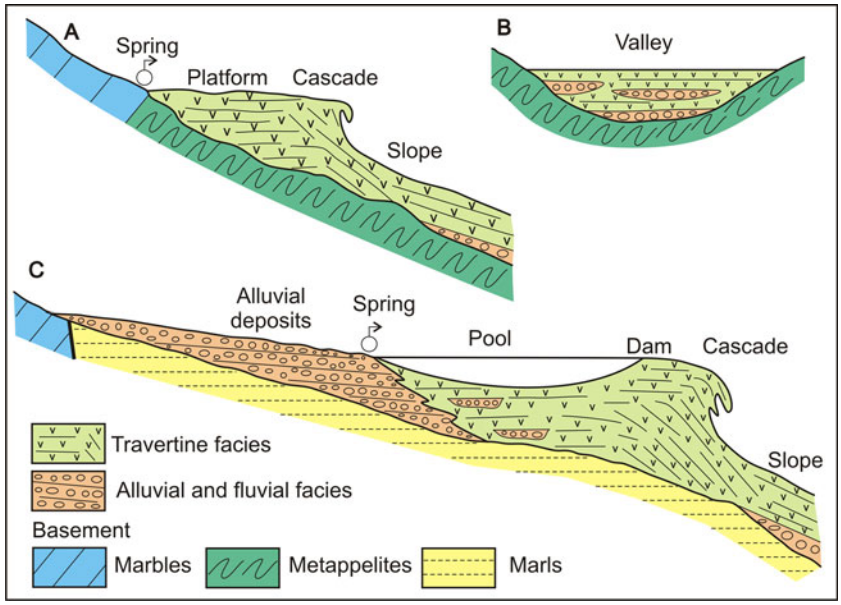


**Figure 10.** (color online) Sedimentary models of the travertines in the western Costa del Sol. (A) Spring-type travertine. (B) Valley-infill model. (C) Pool-dam-cascade model.

Mijas (TM-1) and Alhaurín de la Torre. As in the previous stage, no gastropods were found in relation to the travertine growth of this stage, but Durán et al. (1988) provided an ESR age of 217.0 ± 40 ka for the travertine of Mijas and estimated the age of the travertine of Alhaurín de la Torre at $242.9^{+17.6}/_{-61.0}$ ka based on U/Th dating. The growth of these travertines suggests that the drainage of the Sierra de Mijas changed towards the south (Mijas) and towards the north (Alhaurín de la Torre).

A third stage occurred in the early late Pleistocene when the travertines of Benalmádena (TB-1), Torremolinos (TOR-1), and Churriana (TCH-2) were formed in the Sierra de Mijas that drain towards the south, east, and northeast. The Churriana travertine dates to 88.0 ± 28.2 ka (sample CHU-1) and is similar to Durán's (1996) U/Th series age of $75.4^{+14.8}/_{-13.0}$ ka. In Benalmádena, Durán et al. (1988) dated a travertine with ESR method at 86.3 ± 17 and 109.0 ± 22 ka. The dating of the Torremolinos travertine (TOR-1) is somewhat older (113.7 ± 52.7 ka). All these ages correspond to the early part of the late Pleistocene. In contrast, the dating of Durán et al. (2002) from the Cueva del Bajondillo in the Torremolinos travertine is older at $147.0^{+9.2}/_{-8.5}$ ka and corresponds to the middle Pleistocene. As with those of the second stage, the travertines during the third stage formed at different elevations (190–230 m asl for Benalmádena, 25–50 m asl for Churriana, and 0–25 m asl for Torremolinos).

The greatest development of travertine occurred during the fourth stage in the late Pleistocene: the major building of Mijas (TM-2) is dated to between 52.6 ± 12.4 and 22.6 ± 11.0 ka and Benalmádena (TB-2) to 43.1 ± 16.2 ka. Most of the ages from the Torremolinos travertine can also be included in this stage. Our AAR age of 35.5 ± 6.7 ka from the travertine of Torremolinos is consistent with previous ESR and U/Th dating by Durán et al. (1988), indicating ages between 25.3 ± 5.0 and 27.3 ± 1.7 ka. Also, the TCH-3 growth of Churriana (42.8 ± 18.3 and 28.8 ± 8.5 ka), the travertine of Alhaurín el Grande, with a single U/Th age of $28.7^{+3.0}/_{-2.8}$ ka (Durán, 1996), and the first phase of the TC-2 of the travertine of Coín (39.6 ± 16.7 and 20.3 ± 5.5 ka) offered similar ages. These ages appear to indicate that the Sierra de Mijas maintained drainage predominantly towards the south as well as towards the north, with travertine buildups also appearing at very different heights (350–390 m asl in Mijas; 190–290 m asl in Coín; 180–275 m asl in Alhaurín el Grande; 65–70 m asl in Churriana, and 0–20 m asl in Torremolinos).

A fifth stage of travertine development occurred at the end of the Pleistocene and during the mid-Holocene. This stage is represented by the travertines of Coín (TC-2 high part, 11.6 ± 6.3 and 13.4 ± 14.4 ka) and Churriana (TCH-4, 6.4 ± 6.4 ka), as well as by filling of cavities within the older travertines of Mijas and Alhaurín de la Torre (MIJ-7, 7.9 ± 7.2 ka and ALH-3, 7.2 ± 3.9 ka, respectively). Since the Coín travertine is related to the Sierra Blanca de Coín aquifer (Andreo, 1997), in the mid-Holocene the drainage of the Sierra de Mijas was located towards the Churriana sector. Currently, most of the active springs in the Sierra de Mijas are located along its eastern mountain front between Churriana and Torremolinos (Andreo, 1997).

The chronologic results reveal a significant correlation of the periods of greater travertine growth with the uneven MIS (Fig. 11), corresponding to warm and moist climates, in agreement with previous studies in the Mediterranean and European domains (e.g., Henning et al., 1983; Martínez-Tudela et al., 1986; Ordóñez et al., 1990; Durán, 1996; Torres et al., 1996, 2005; García del Cura et al., 1996; Kronfeld et al., 1988; Frank et al., 2000; Peña et al., 2000; Martín-Algarra

https://doi.org/10.1017/qua.2018.128 Published online by Cambridge University Press

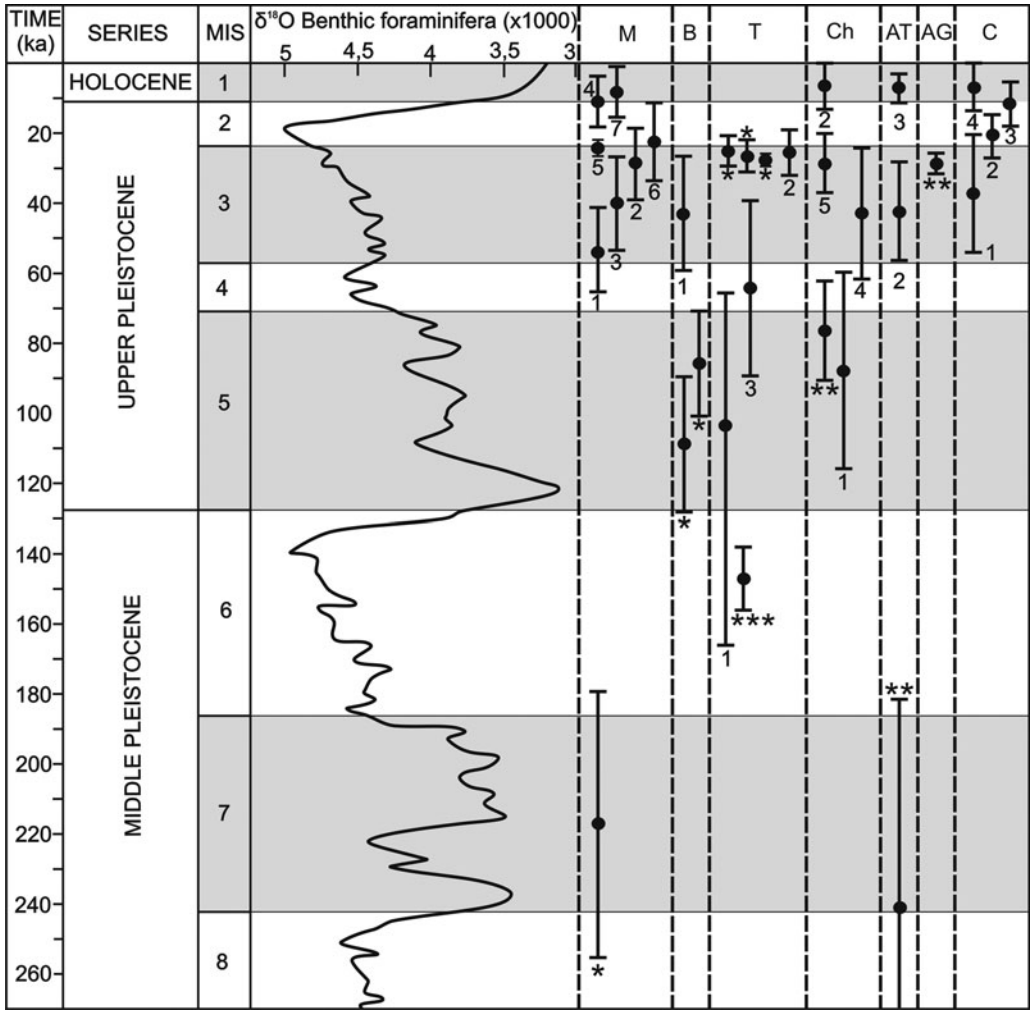


**Figure 11.** (color online) Chronology of the travertines of the western Costa del Sol. Correlation with the values of $\partial^{18}O$ of the benthic foraminifera from Lisiecki and Raymo (2005) and the Marine Oxygen Isotope Stages (MIS). M: Mijas; B: Benalmádena; T: Torremolinos; Ch: Churriana; AT: Alhaurín de la Torre; AG: Alhaurín el Grande; C: Coín. * Dates of Durán et al. (1988); ** Dates of Durán (1996); *** Dates of Durán et al. (2002).

et al., 2003; Ortiz et al., 2009). The first stage of travertine formation (TCH-1) remains too undefined to assign it to one or several specific isotope episodes. We can only estimate that this travertine started to develop in the region at a stage prior to the MIS 9. A more-defined second episode appears to correlate temporally with MIS 7 (middle Pleistocene) during which the travertines began to grow in Mijas and Alhaurín de la Torre. The travertines of Benalmádena and Churriana of the third episode formed during MIS 5 (earliest late Pleistocene), while that of Torremolinos could continue forming during the late part of MIS 6, according to the dating by Durán et al. (2002). The widespread travertine development of the fourth episode occurred mainly during the MIS 3 and beginning of the MIS 2 (latest Pleistocene). The youngest part of the travertines of Coín (TC-2 high part) and Churriana (TCH-4) developed in the fifth episode at the end of MIS 2 and during the Holocene (MIS 1).

As a whole, the ages and altitudes of the studied travertines reveal that there is no close relationship between these two parameters. The height of the travertines mainly depends on the location of the marble/pelite contact. However, the travertines are at higher elevations westwards, as well as the remains of the early Pliocene marine abrasion platform (400–360 m asl between Coín and Alhaurín el Grande; 350–290 m asl in the Alhaurín de la Torre; and 200–260 m asl in the sector between Churriana and Torremolinos). Accordingly, as previously noted by Sanz de Galdeano and López Garrido (1991), Insua-Arévalo (2008), and Guerra-Merchán et al. (2018), the Sierra de Mijas has undergone progressively greater uplifting westwards since the late Pliocene.

## CONCLUSIONS

The carbonate nature of the Sierra de Mijas and other minor sierras of the western Costa del Sol, in addition to a poorly-permeable pelite basement, has favored the presence of abundant springs of calcareous water, allowing the development of

https://doi.org/10.1017/qua.2018.128 Published online by Cambridge University Press

travertine buildups throughout the Pleistocene and Holocene. Four major types of facies characterize the travertine buildups: (1) facies bioconstructed by abundant remains of higher plants, usually small- and medium-sized stems, in horizontal or slightly-inclined layers; (2) facies bioconstructed by stems frequently of great size, which dispose in irregular, subvertical beds; (3) oncolite facies; and (4) botryoidal and globular stromatolite facies.

The location of the fountainheads, the associations of facies, and the geomorphic characteristics allow assigning the travertine buildups to three previously defined models:

(a) spring-type travertines, usually located on the southern edge of the Sierra de Mijas (TM-1, travertine of Osunilla of the TM-2 in Mijas, and TB-1 in Benalmádena). These travertines developed on a mountainous carbonate basement close to the contact with metapelites where fountains or springs are frequent.
(b) valley-type travertines located in Mijas (TM-2), Benalmádena (TB-2), and Churriana (TCH-3), as a result of the gully filling incised in older travertines or in the basement.
(c) pool-dam-cascade-type travertines recognized in the Torremolinos, Churriana, Alhaurín de la Torre, and Alhaurín el Grande areas. These usually large travertines appear overlying Pliocene deposits far from the marble basement.

The presence of Helicidae gastropods in the travertine buildups has allowed the obtainment of a series of AAR ages that improve constraints on the timing of travertine buildups. Most travertines are polyphasic and the greater development occurred during the warm and moist interglacial/interstadial, i.e., MIS 7, 5, 3, and 1. Nevertheless, local travertine growth may have also occurred during parts of the glacial/stadial (e.g., in Torremolinos during MIS 4 and 6 and in Mijas and Coín in the transition from MIS 3 to 2).

The study of the travertines of the western Costa del Sol advances the knowledge of the development of the Quaternary travertines in the Mediterranean realm, revealing that their growth preferentially occurs during hot and humid periods (uneven MIS). In addition, the development of the travertines is frequently polyphasic, with intermediate erosive stages.

## SUPPLEMENTARY MATERIAL

The supplementary material for this article can be found at https://doi.org/10.1017/qua.2018.128.

## ACKNOWLEDGMENTS

This study was supported with funding provided by Research Group RNM-146 of the "Junta de Andalucía" and project CGL2016-78577-P of the Spanish Ministry of Science and Innovation. We appreciate the interesting criticisms and remarks done by the editors Dr. Lewis Owen and Dr. Jeff Pigati, as well as by the reviewers Dr. Brent Koppel and Dr. Martín-Algarra, who helped improve this paper. We also wish to thank Mr. David Nesbitt for the English revision of the manuscript.

.

## REFERENCES

Andreo, B., 1997. Hidrogeología de acuíferos carbonatados en las Sierras Blanca y Mijas (Cordillera Bética, Sur de España). Servicio de Publicaciones de la Universidad de Málaga, Málaga.

Andreo, B., Sanz de Galdeano, C., 1994. Structure of the Sierra de Mijas (Alpujarride Complex, Betic Cordillera). *Annales Tectonicae* 8, 23–35.

Bates, R.L., Jackson, J.A., 1987. *Glossary of Geology*. 3rd ed. American Geological Institute, Alexandria, VA.

Bragado, M.D., Araujo, R., Aparicio, M.T., 2009. *Atlas y libro rojo de los moluscos de Castilla-La Mancha*. Organismo Autónomo de Espacios Naturales de Castilla-La Mancha, Guadalajara.

Chen, D., Chen, H.W., 2013. Using the Köppen classification to quantify climate variation and change: An example for 1901–2010. *Environmental Development* 6, 69–79.

Clark, I.A., Fontes, J.Ch., 1990. Paleoclimatic Reconstruction in Northern Oman Based on Carbonates from Hyperalkaline Groundwaters. *Quaternary Research* 33, 320–336.

Clark, I.D., Khoury, H.N., Salameh, E., Fritz, P., Göksu, H.Y., Wiesser, A., Fontes, J.Ch., Causse, C., 1991. Travertines in Central Jordan: implications for palaeohydrology and dating. Proceedings of the International Atomic Energy Agency Symposium SM-319. The Use of Isotope Techniques in Water Resources Development. Vienna, Austria, March 11–15, 1991.

Delgado Castilla, L., 2009. Edades U/Th de los travertinos del cuaternario reciente de la Cuenca de Tabernas, Almería: implicaciones en su evolución geodinámica y paleoambiental. *Cuaternario y Geomorfología* 23, 65–76.

Durán, J.J., 1996. Los sistemas kársticos de la provincia de Málaga y su evolución: contribución al conocimiento paleoclimático del Cuaternario en el Mediterráneo occidental. PhD dissertation, Complutense University of Madrid, Spain.

Durán, J.J., Grün, R., Soria, J., 1988. Edad de las formaciones travertinas del flanco meridional de la Sierra de Mijas (provincia de Málaga, Cordilleras Béticas). *Geogaceta* 5, 61–63.

Durán, J.J., Carrasco, F., Andreo, B., Marqués, I., Baldomero, A., Ferrer, I.E., Cortés, M., 2002. Aspectos cronoestratigráficos de los travertinos de Torremolinos (Málaga, Sur de España), a partir de nuevos datos del yacimiento arqueológico del Bajondillo. In: Carrasco, F., Durán, J.J., Andreo, B. (Eds.), *Karst and Environment*. Fundación Cueva de Nerja, Málaga, pp. 465–470.

Eikenberg, J., Vezzu, G., Zumsteg, I., Bajo, S., Ruethi, M., Wyssling, G., 2001. Precise two chronometer dating of Pleistocene travertine: the 230Th/234U and 226Ra/226Ra (0) approach. *Quaternary Science Reviews* 20, 1935–1953.

Engin, B., Güven, O., 1997. Thermoluminescence dating of Denizli travertines from the southwestern part of Turkey. *Applied Radiation and Isotopes* 48, 1257–1264.

Ford, T.D., Pedley, H.M., 1992. Tufa deposits of the world. *Journal of the Speleological Society of Japan* 17, 46–63.

Ford, T.D., Pedley, H.M., 1996. A review of tufa deposits of the world. *Earth-Science Reviews* 41, 117–175.

Frank, N., Braum, F.N., Hambach, M., Mangini, A., Wagner, G., 2000. Warm period growth of travertine during the last interglaciation in southern Germany. *Quaternary Research* 54, 38–48.

García del Cura, M.A., González, J.A., Ordóñez, S., Pedley, M., 1996. Las Lagunas de Ruidera. In: García, J.L., González, E. (Eds.), *Elementos del Medio Natural en la provincia de Ciudad Real*, Universidad de Castilla-La Mancha, pp. 84–129.

García-García, F., Nieto, L.M., 2005. El sistema aluvio-travertínico de Frailes (Cuenca Neógeno-Cuaternaria de Alcalá la Real, provincia de Jaén, Cordillera Bética). *Geogaceta* 37, 75–78.

González Martín, J.A., González Amuchastegui, M.J., 2014. *Las Tobas en España*. Sociedad Española de Geomorfología, Badajoz, España.

Goodfriend, G.A., 1991. Patterns of racemization and epimerization of amino acids in land snail shells over the course of the Holocene. *Geochimica et Cosmochimica Acta* 55, 293–302.

Goodfriend, G.A., Meyer, V., 1991. A comparative study of the kinetics of amino acid racemization/epimerization in fossil and modern mollusc shells. *Geochimica et Cosmochimica Acta* 55, 3355–3367.

Grün, R., Schwarcz, H.P., Ford, D.C., Hentzsch, B., 1988. ESR dating of spring deposited travertine. *Quaternary Science Reviews* 7, 429–432.

Guerra-Merchán, A., Serrano, F., Ramallo, D., 2000. El Plioceno de la Cuenca de Málaga (Cordillera Bética). *Geotemas* 1, 108–110.

Guerra-Merchán, A., Serrano, F., Hlila, R., Kadiri, K., Sanz de Galdeano, C., Garcés, M., 2014. Tectono-sedimentary evolution of the peripheral basins of the Alboran Sea in the arc of Gibraltar during the latest Messinian-Pliocene. *Journal of Geodynamics* 77, 158–170.

Guerra-Merchán, A., Serrano, F., García-Aguilar, J.M., Sanz de Galdeano, C., Ortiz, J.E., Torres, T., Sánchez-Palencia, Y., 2018. The Late Cenozoic landscape development in the westernmost Mediterranean (southern Spain). Geomorphology https://doi.org/10.1016/j.geomorph.2018.11.008.

Hearty, P.J., O'Leary, M.J., Kaufman, D.S., Page, M.C., Bright, J., 2004. Amino acid geochronology of individual foraminifer (Pulleniatina obliquiloculata) tests, north Queenland margin, Australia: a new approach to correlating and dating Quaternary tropical marine sediment cores. *Paleoceanography* 19, PA4022.

Hennig, G.J., Grünn, R., Brunnacker, K., 1983. Speleothems, travertines, and paleoclimates. *Quaternary Research* 20, 1–29.

Hillarie-Marcel, C., Carro, O., Casanova, J., 1986. $^{14}C$ and Th/U dating of Pleistocene and Holocene stromatolites from East African paleolakes. *Quaternary Research* 25, 312–329.

Hubbard, D.A., Herman, J.S., 1990. Overview of travertine-marl volumen. In: Herman, J.S. and Hubbard, D.A. (Eds.), *Travertine-marl: stream deposits in Virginia*. Virginia Division of Mineral Resources Publication 101:1–4.

Insua-Arévalo, J.M., 2008. Neotectónica y Tectónica Activa de la Cuenca de Málaga (Cordillera Bética Occidental). PhD dissertation, Universidad Complutense de Madrid, Spain.

Insua-Arévalo, J.M., Martínez-Díaz, J.J., García-Mayordomo, J., Martín-García, F., Capote, R., 2007. *Los abanicos aluviales del borde norte de la Sierra de Mijas (Cuenca de Málaga, Cordillera Bética occidental)*. XII Reunión Nacional de Cuaternario, Ávila, pp. 151–152.

Insua-Arévalo, J.M., Martínez-Díaz, J.J., García-Mayordomo, J., Martín-González, F., 2012. Active tectonics in the Málaga Basin: evidences from morphotectonic markers (western Betic Cordillera, Spain). *Journal of Iberian Geology* 38, 175–190.

Juliá, R., 1983. Travertines. In: Scholle, P.A., Bebout, D.G., Moore, C.H. (Eds.), *Carbonate Depositional Environments*. American Association of Petroleum Geologists Memoir 33, 62–72.

Kaufman, D.S., 2000. Amino acid racemization in ostracodes. In: Goodfriend, G., Collins, M., Fogel, M., Macko, S., Wehmiller, J. (Eds.), *Perspectives in Amino Acid and Protein Geochemistry*. Oxford University Press, New York, pp. 145–160.

Kaufman, D.S., 2003. Amino acid paleothermometry of Quaternary ostracodes from the Bonneville Basin, Utah. *Quaternary Science Reviews* 22, 899–914.

Kaufman, D.S., 2006. Temperature sensitivity of aspartic and glutamic acid racemization in the foraminifera *Pulleniatina*. *Quaternary Geochronology* 1, 188–207.

Kaufman, D.S., Manley, W.F., 1998. A new procedure for determining DL amino acid ratios in fossils using reverse phase liquid chromatography. *Quaternary Geochronology* 17, 987–1000.

Koban, C.G., Schweigert, G., 1993. Microbial origin of travertine fabrics: two examples from southern Germany (Pleistocene Stuttgart travertine and Miocene Riodöschingen travertine). *Facies* 29, 251–264.

Kosnik, M.A., Kaufman, D.S., 2008. Identifying outliers and assessing the accuracy of amino acid racemization measurements for geochronology: II. *Data screening*. Quaternary Geochronology 3, 328–341.

Kronfeld, J., Vogel, J.C., Rosenthal, E., Weinstein-Evron, M., 1988. Age and paleoclimatic implications of Bet Shean travertines. *Quaternary Research* 30, 298–303.

Laabs, B.J.C., Kaufman, D.S., 2003. Quaternary highstands in Bear Lake Valley, Utah and Idaho. *Geological Society of America Bulletin* 115, 463–478.

Lisiecki, L.E., Raymo, M.E., 2005. A Pliocene-Pleistocene stack of 57 globally distributed benthic $\delta^{18}O$ records. *Paleoceanography* 20, PA1003, 1–17.

Magnin, F., Guendon, J.L., Vaudour, J., Martin, Ph., 1991. Les travertins: accumulations carbonatées associées aux systémes karstiques, séquences sédimentaires et paléo-environnements quaternaires. *Bulletin Société Géologique de France* 162, 585–594.

Martín-Algarra, A., Martín-Martín, M., Andreo, B., Julià, R., González-Gómez, C., 2003. Sedimentary patterns in perched spring travertines near Granada (Spain) as indicators of the paleohydrological and paleoclimatological evolution of a karst massif. *Sedimentary Geology* 161, 217–228.

Martínez-Tudela, A., Cuenca, F., Santisteban, C., Grun, R., Hentzsch, B., 1986. Los travertinos del Rio Matarraña, Beceite (Teruel) como indicadores paleoclimáticos del Cuaternario. In: López-Vera, A. (Ed.), *Quaternary Climate in Western Mediterranean*, pp. 307–324.

Mollat, H., 1968. Schichtenfolge un tektonisher Bau der Sierra Blanca und ihrer Umgebung (Betische Kordilleren, Südspanien). *Geologisches Jahrbuch* 86, 471–521.

Murray-Wallace, C.V., 1995. Aminostratigraphy of Quaternary coastal sequences in southern Australia: an overview. *Quaternary International* 26, 69–86.

Ordóñez, S., González, J.A., García del Cura, M.A., 1990. Datación radiogénica (U-234/U-238 y Th-230/U-234) de sistemas travertínicos del Alto Tajo (Guadalajara). *Geogaceta* 8, 53–56.

Ortiz, J.E., Torres, T., Delgado, A., Reyes, E., Díaz-Bautista, A., 2009. A review of the Tagus river tufa deposits (central Spain): age and palaeoenvironmental record. *Quaternary Science Reviews* 28, 947–963.

Ortiz, J.E., Torres, T., Pérez-González, A., 2013. Amino acid racemization in four species of ostracodes: taxonomic, environmental, and microstructural controls. *Quaternary Geochronology* 16, 129–143.

Pedley, H.M., 1990. Classification and environmental models of cool freshwater tufas. *Sedimentary Geology* 68, 143–154.

Penkman, K.E.H., Preece, R.C., Keen, D.H., Maddy, D., Schreve, D.S., Collins, M.J., 2007. Testing the aminostratigraphy of fluvial archives: the evidence from intra-crystalline proteins within freshwater shells. *Quaternary Science Reviews* 26, 2958–2969.

Penkman, K.E.H., Kaufman, D.S., Maddy, D., Collins, M.J., 2008. Closed-system behaviour of the intra-crystalline fraction of amino acids in mollusk shells. *Quaternary Geochronology* 3, 2–25.

Pentecost, A., 1993. British travertines: a review. *Proceedings of the Geologists Association* 104, 23–39.

Pentecost, A., 1995. The Quaternary travertine deposits of Europe and Asia Minor. *Quaternary Science Reviews* 14, 1005–1028.

Pentecost, A., 2005. *Travertine*. Springer-Verlag, Berlin and Heidelberg, Germany.

Pentecost, A., Viles, H.A., 1994. A review and reassessment of travertine classification. *Géographie Physique et Quaternaire* 48, 305–314.

Peña, J.L., Sancho, C., Lozano, M.V., 2000. Climatic and tectonic significance of Late Pleistocene and Holocene tufa deposits in the Mijares river canyon, eastern Iberian range, northeast Spain. *Earth Surface Processes and Landforms* 25, 1403–1417.

Piles Mateo, E., Estévez González, C., Barba Martín, A., 1978. *Hoja y memoria explicativa de la Hoja de Coín-1066 del Mapa Geológico de España a escala 1:50.000*. Instituto Geológico y Minero de España, Madrid.

Reddmann, Th., Schüttlekopf, H., 1986. Thermoluminescence dating of Pleistocene travertine. *Radiation Protection Dosimetry* 17, 1–4.

Riding, R., 1991. Classification of microbial carbonates. In: Riding, R. (Ed.), *Calcareous Algae and Stromatolites*. Springer-Verlag, Berlin, pp. 21–51.

Rivas-Martínez, S., Rivas-Sáenz, S., 2009. Worldwide Bioclimatic Classification System (accessed April 15, 2018). www.globalbioclimatics.org.

Rodrigo Comino, J., Senciales González, J.M., 2012. Las plataformas travertínicas y tobáceas de la provincia de Málaga (España). *Baetica.* Estudios de Arte, Geografía e Historia 34, 83–102.

Rodríguez-Vidal, J., Abad, M., Cáceres, L.M., González-Regalado, M.L., Lozano-Francisco, M.C., Ruiz, F., Vera-Peláez, J.L., Cortés Sánchez, M., de la Rubia de Gracia, J.J., Simón Vallejo, M.D., 2007. Rasgos morfosedimentarios del piedemonte nororiental de la Sierra de Mijas (Torremolinos, Málaga). In: Cortés Ramos, M. (Ed.), *Cueva Bajoncillo (Torremolinos).* Secuencia cronocultural y paleoambiental del Cuaternario reciente en la Bahía de Málaga. Servicio de Publicaciones del Centro de Ediciones de la Diputación de Málaga, Málaga, pp. 25–35.

Rubel, F., Kottek, M., 2010. Observed and projected climate shifts 1901–2100 depicted by world maps of the Köppen-Geiger climate classification. *Meteorologische Zeitschrift* 19, 135–141.

Sánchez-Goñi, M.F., Eynaud, F., Turon, J.L., Shackleton, N.J., 1999. High resolution palynological record off the Iberian margin: direct land-sea correlation for the last interglacial complex. *Earth and Planetary Science Letters* 171, 123–137.

Sánchez-Goñi, M.F., Cacho, I., Turon, J.L., Guiot, J., Sierro, F.J., Peypouquet, J.P., Grimalt, J., Shackleton, N.J., 2002. Synchroneity between marine and terrestrial responses to millenial scale climatic variability during the last glacial period in the Mediterranean region. *Climate Dynamics* 19, 95–105.

Sánchez-Goñi, M.F., Landais, A., Fletcher, W.J., Naughton, F., Desprat, S., Duprat, J., 2008. Contrasting impacts of Dansgaard-Oeschger events over a western European latitudinal transect modulated by orbital parameters. *Quaternary Science Reviews* 27, 1136–1151.

Sanz de Galdeano, C., 1997. La Zona Interna Bético-Rifeña: antecedentes, unidades tectónicas, correlaciones y bosquejo de reconstrucción paleogeográfica. *Monográfica Tierras del Sur*. Universidad de Granada, Granada.

Sanz de Galdeano, C., López Garrido, A.C., 1991. Tectonic evolution of the Málaga Basin (Betic Cordillera). *Regional implications.* Geodinamica Acta 5, 173–186.

Soligo, M., Tuccimei, P., Barberi, R., Delitala, M.C., Miccadei, E., Taddeucci, A., 2002. U/Th dating of freshwater travertine from Middle Velino Valley (Central Italy): paleoclimatic and geological implications. *Palaeogeography, Palaeoclimatology, Palaeoecology* 184, 147–161.

Srdoč, D., Horvatinčić, N., Obelić, B., Sliepčević, A., 1983. Radiocarbon dating of tufa in paleoclimatic studies. *Radiocarbon* 25, 421–428.

Torres, T., Llamas, J., Canoira, L., García-Alonso, P., García-Cortés, A., Mansilla, H., 1995. Amino chronology of the lower Pleistocene deposits of Venta Micena, Orce, Granada. In: Grimalt, J. O., Dorronsoro, C. (Eds.), *Organic Geochemistry: Developments and Applications to Energy, Climate, Environment and Human History*. ALAGO, San Sebastián, pp. 722–724.

Torres, T., Cobo, R., Canoira, L., García Cortés, A., Grün, R., Hoyos, M., Juliá, R., *et al*., 1996. Aportaciones al conocimiento de la evolución paleoclimática y paleoambiental en la península Ibérica durante los dos últimos millones de años a partir del estudio de travertinos y espeleotemas. Empresa Nacional de Residuos Radioactivos, S.A., Publicación técnica 3/96. 118 pp.

Torres, T., Llamas, J., Canoira, L., García-Alonso, P., García-Cortés, A., Mansilla, H., 1997. Amino acid chronology of the lower Pleistocene deposits of Venta Micena (Orce, Granada, Andalusia, Spain). *Organic Geochemistry* 26, 85–97.

Torres, T., Llamas, J., Canoira, L., García-Alonso, P., Ortiz, J.E., 1999. Estratigrafía Biomolecular. *La racemización/epimerización de aminoácidos como herramienta geocronológica y paleotermométrica*. ENRESA, Madrid.

Torres, T., Ortiz, J.E., García de la Morena, M.A., Llamas, F.J., Goodfriend, G., 2005. Aminostratigraphy and aminochronology of a tufa system in central Spain. *Quaternary International* 135, 21–33.

Tubía, J.M., 1985. Estructura de los Alpujárrides occidentales: cinemática y condiciones de emplazamiento de las peridotitas de Ronda. PhD dissertation, Universidad del País Vasco, España.

Whitten, D.A., Brooks, J.V.R., 1972. *The Penguin Dictionary of Geology*. Penguin, London.

https://doi.org/10.1017/qua.2018.128 Published online by Cambridge University Press